JOURNAL OF MATERIALS SCIENCE 24 (1989) 4403–4408

Pore size distribution, grain growth, and the sintering stress

LUTGARD. C. DE JONGHE, MAY-YING CHU, MARK K. F. LIN
Department of Materials Science and Mineral Engineering and Center for Advanced Materials, Lawrence Berkeley Laboratory, University of California, Berkeley, California 94720, USA

The effects of a pore size distribution and of the pore separation on the sintering stress is examined using a simple model. The sintering stress is found to be proportional to the mean of the pore sizes weighted according to the Voronoi cell pertaining to each pore, rather than to the simple pore size average. Large heteropores are shown to have little effect on the mean effective sintering stress. Decreases in pore coordination number of such pores, resulting from grain growth can significantly increase the stress intensification factor. The near-constancy of the sintering stress, observed experimentally for many powders over a wide range of sintered densities, does not directly follow from the simple model. It is argued that this constancy results from pore shrinkage, due to densification, which is compensated by pore growth due to coarsening.

1. Introduction

Practical powder compacts contain imperfections that affect their microstructural development and their sintering behaviour very significantly. These imperfections are well known but very difficult to avoid completely: inhomogeneous particle and pore distributions, either in the green powder compact or developing as a result of abnormal grain growth and pore break away, are the source of many of the undesirable features in sintered bodies.

In considering the densification process of heterogeneous powder compacts, the presence of inhomogeneities must be taken into account and considered together with grain growth or coarsening to reach an understanding of the sintering process. An important parameter in characterizing densification is the sintering stress [1], Σ/ϕ, (also called the sintering force [2], the sintering potential [3], or the sintering pressure [4]) where Σ is the mean stress on the grain boundaries or in the skeleton of solids and ϕ is the ratio of overall cross-sectional area to load bearing area, and how it is affected by coarsening or grain growth and by the presence of a pore size distribution. The present paper attempts to elucidate these processes by examining simple models of pore distributions and relating these to experimental determinations of the sintering stress.

Several investigators have considered the evolution and the role of microstructure, and its effects on sintering of powder compacts. Perhaps the first ones to emphasize this aspect of densification were Rhines and his coworkers [1, 5], who focussed on the structural evolution of the pore network, when most other researchers were attempting to correlate diffusion data from traditional tracer diffusion experiments with those extracted from sintering of powder compacts. These comparisons most often used highly abstracted representations, such as the two-sphere model, in the data analysis [6, 7]. Gregg and Rhines [8] departed from this direction and attempted to measure the sintering stress (or sintering force) from zero-strain rate conditions observed during tensile loading of sintering copper compacts. Generally, for these copper sphere compacts, the sintering stress increased with increasing density. These authors successfully correlated the measured sintering stress with the quantitative stereological data obtained on their specimens. More recently, De Jonghe *et al* [9], and Raj *et al* [4] used a different, and perhaps somewhat simpler, experimental technique to determine the sintering stress. The simultaneous measurement of creep and densification led to the interesting observation on all ceramic powder systems studied so far that, at constant applied stress, the ratio of the densification strain rate over the creep strain rate is constant *from the onset of densification*, over a wide range of sintered densities. This finding, indicating that the sintering stress is constant, is in contrast to the earlier observations of Gregg and Rhines who found the sintering stress for copper sphere compacts to increase monotonically for most of the same density range. In this paper some possible reasons are offered that may explain this difference in evolution of the measured sintering stresses.

Effects of particle size distribution on densification rates were analysed by Coble [10], who treated this problem by taking into account the effects of the strain rate mismatch associated with the different local unconstrained sintering rates of particle pairs. Here, a related procedure is followed to solve for the densification strain rate of stress-coupled pore assemblies. Formal consideration of the importance of the back-stresses generated by differential densification that results from heterogeneous regions of inclusions in powder compacts was presented by Hsueh *et al* [3], by Raj *et al* [4, 11], and by Scherer [12]. These treatments considered explicitly the interaction of the mismatch

0022–2461/89 $03.00 + .12

backstresses with the sintering stress. An experimentally based analysis by De Jonghe *et al* [1], and a study by Scherer [13] showed that these backstresses were simply viscous, and that viscoelastic stresses do not accumulate in a sintering body. Therefore, the time-dependent viscoelastic problem need not be solved, and quasi-steady state conditions can be assumed when formulating the instantaneous self stress in densification of heterogeneous powder compacts.

The relationship between the sintering stress, which is the equivalent externally applied stress, and the effective mean stress on the grain boundaries follows from a geometrical analysis. In general, this analysis would be complex. Beeré [14, 15] considered this relationship for uniform pore networks equilibrated at some fixed densities, and defined the stress intensification factor, ϕ, as providing the relationship. Vieira and Brook [16] fitted these calculations to an exponential expression, which was later verified experimentally by Rahaman *et al* [17] in a set of creep-sintering experiments. The presence of large heteropores in a fine-pore matrix can both affect ϕ as well as the sintering stress. The model used here considered the effects of large heteropores on the sintering stress and on the stress intensification factor, ϕ.

Practically, the importance of non-uniformity in powder compacts in obstructing the production of high quality sintered products has been well documented. For example, Rhodes [18] studied the effects of agglomeration on sintering, and made the important observation that the full potential of fine powders can only be realized when agglomerates are eliminated. The full significance of this observation was later made evident by the use of near-monosized powders by Pober *et al* [19]. In another example, Dynys and Halloran [20] demonstrated that the densification rate of a green compact decreases with increasing agglomerate content. For some ZnO powder compacts containing dispersions of SiC particles, De Jonghe and Rahaman [21] demonstrated a significant reduction in the sintering rates compared to single-phase compacts, as the volume fraction of inclusions increased. The severity of this reduction in sintering rates of particulate composites increased with decreasing dispersed particle size, an effect not predicted by a viscous or viscoelastic analysis, which could be attributed in part to the increased tendency of the dispersed phase to cluster as its particle size decreases. One form of cluster formation was addressed by Lange [22] who considered the possible development of undeformable percolation skeletons by the dispersed phase. Lange and Davis [23] also reported on the sintering of agglomerated powder compacts and discussed the possible role of the pore coordination number, concluding that grain growth may have to preceed densification if this number is too high. The effects of the pore coordination number and the presence of isolated large pores is also considered here and related to the sintering stress.

2. Model

To examine the behaviour of a pore distribution, a one-dimensional model, as shown in Fig. 1, is adopted.

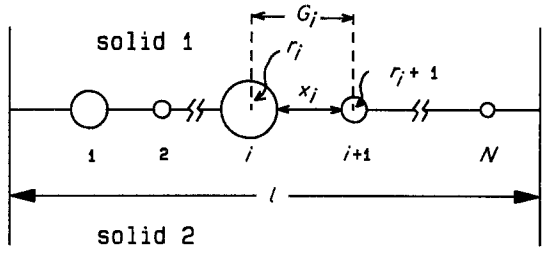

Figure 1 One-dimensional model of a string of N pores contained in a length l between two solids.

A string of N pores is contained in length l of grain boundary between two solids. The ith pore has a radius r_i and is separated from the $(i + 1)$th pore by the grain boundary segment of length x_i. The overall stress intensification factor ϕ for this system is simply

$$\phi = l \Big/ \sum_1^N x_i \tag{1}$$

while the stress intensification factor of the ith unconstrained segment is

$$\phi_i = G_i/x_i \tag{2}$$

(It is noted here that $\phi \equiv \Sigma_1^N G_i/\Sigma_1^N x_i$ which does not equal $\Sigma_1^N (G_i/x_i)$.)

The effective sintering stress on x_i, that is the mean stress exerted on the free segment x_i, is

$$\Sigma_i = \gamma\phi_i(1/r_i + 1/r_{i+1})/2 \tag{3}$$

(The effects of the grain boundaries, introducing a grain size dependent term in Equations 1 and 2, as discussed by Cannon [3] and by De Jonghe and Rahaman [1], is ignored here. It could, in principle, be accommodated by choosing an effective r_i that is slightly different from the physical one.)

The constrained displacement rate of the ith segment is then

$$\dot{s}_i = K(\Sigma_i + \sigma_i/\gamma)/x_i^2 \tag{4}$$

where K is a kinetic constant and σ_i are the compatibility stresses that are needed to have the displacement rate equal for each segment to the overall displacement rate $\dot{s}$. Since the σ_i are self-stresses they must obey

$$\sum_1^N \sigma_i x_i = 0 \tag{5}$$

Multiplying both sides in Equation 4 with x_i^3 and summing then gives

$$\dot{s} = K\left(\sum_1^N \Sigma_i x_i\right) \Big/ \sum_1^N x_i^3 \tag{6}$$

$\Sigma_i x_1$ is also the force exerted on the unconstrained ith segment, so that with Equation 5 the total force, F, exerted on the boundary of length l is

$$F = \sum_1^N F_i = \sum_1^N \Sigma_i x_i \tag{7}$$

Also, by definition one has

$$\sum_1^N F_i/l \equiv \Sigma/\phi \tag{8}$$

From Equations 1 to 3, 6 and 7 it follows that

$$\Sigma = \gamma \left(\sum_{1}^{N} [(G_i + G_{i+1})/2](1/r_i) \right) \Big/ \sum_{1}^{N} x_i \quad (9)$$

if it is assumed that the first and the last term of the summation have little effect on the total sum. This becomes a good approximation for N sufficiently large. With $\langle\ \rangle$ denoting the arithmetical average, Equation 9 may be written as

$$\Sigma = \gamma \langle G_i/r_i \rangle / \langle x_i \rangle \quad (10)$$

Equation 10 establishes the relationship between the details of the microstructure of the model and the macroscopic value of the effective sintering stress, Σ. If G_i and r_i are statistically uncorrelated then one has

$$\langle G_i/r_i \rangle = \langle G_i \rangle \langle 1/r_i \rangle \quad (11)$$

so that, from Equations 2 and 10, it would follow that

$$\gamma[\langle G_i \rangle / \langle x_i \rangle] \langle 1/r_i \rangle = \gamma \phi \langle 1/r_i \rangle \quad (12)$$

Then, one would obtain the usual expression for the driving force of sintering, Σ/ϕ, as the mean curvature of the pores. Equation 11 indicates, however, that this result is only valid if the pore spacing and the pore radii are statistically strictly independent. This is very unlikely to be satisifed in any powder compact. For example, a large heteropore is separated from its smaller neighbours by approximately the particle size, as is evident in the partly sintered microstructure shown in Fig. 2a. Equation 9 may also be written as follows, if end effects are again ignored in the summation

$$\Sigma = \gamma \sum_{1}^{N} [(G_i + G_{i+1})/2](1/r_{i+1})/N\langle x_i \rangle \quad (13)$$

The term $(G_i + G_{i+1})/2$ has the same meaning as the Voronoi cell pertaining to the $(i + 1)$th pore. In general then, the value of the sintering stress will *not* correspond to the mean curvature of the pores as derived, for example from a stereological analysis; rather the curvature of the pores will need to be weighted according to the size of their associated Voronoi cell. This makes the derivation of a valid sintering stress from quantitative microscopy far more difficult, except in those cases where the validity of Equation 11 can be clearly established.

The quantitative extension of the argument to an irregular, continuous three-dimensional pore network is not straightforward, since Voronoi cells cannot be constructed readily. It should, however, be expected that the macroscopic sintering stress will again depend on pore curvature weighted by a measure of local pore separation.

3. Effects of isolated large pores

Isolated large pores are often present in green or partly sintered powder compacts. As an example, a partly sintered, heterogeneous powder compact of MgO is shown in Figs 2a and 2b. The effects of the presence of a limited number of large pores in a fine-pore matrix on the sintering stress and on the stress intensification factor can, in part, be assessed by considering a modified version of Fig. 1. In the original

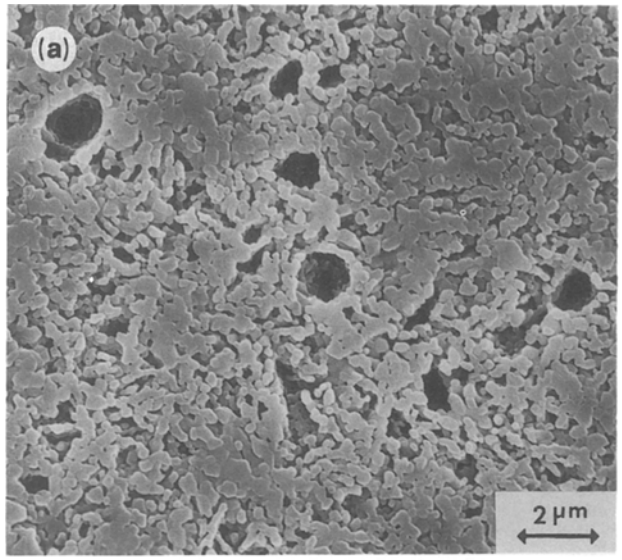

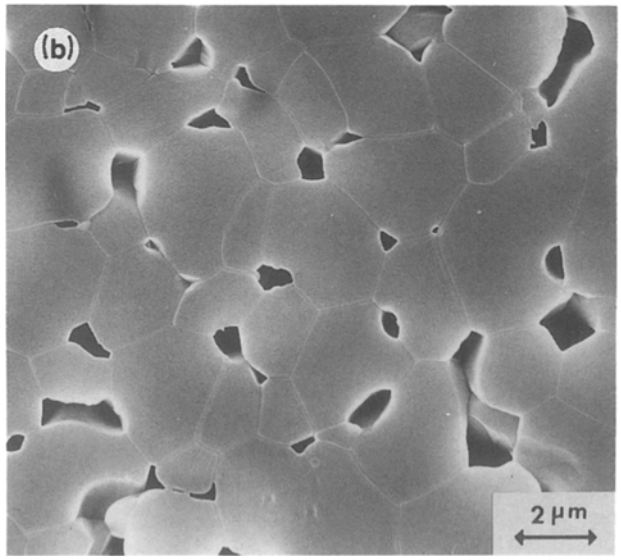

Figure 2 (a) Microstructure of partly sintered MgO compact, bimodal pore structure (polished surface). (b) Microstructure of MgO compact upon further sintering, more uniform pore structure (polished surface).

pore distribution, Fig. 3a, containing N pores, a large pore of radius r_L is inserted to replace a small one where $r_L \gg r$, Fig 3b. This changes l to $(l + 2r_L)$ and, replaces one term with $(G_L + G_{L+1})/2r_L$ in the summation, Equation 9. In this procedure the x_i are unchanged. If relatively few large pores are substituted, the isolated, large heteropores would hardly affect the magnitude of the effective sintering stress ε. Significant decreases in the effective sintering stress ε, might result if the large pore would, at the same time, have large nearest neighbour spacings, but this would be an uncommon situation. As an example, the microstructure shown in Fig. 2a indeed shows no such correlation between the spacing to the pores neighbouring the large pores and the large pore radius.

The value of the stress intensification factor, ϕ, would, however, be affected in proportion to the increase in grain boundary porosity. If the stress intensification factor before introduction of the large pore is ϕ_i and after the introduction of the large pore

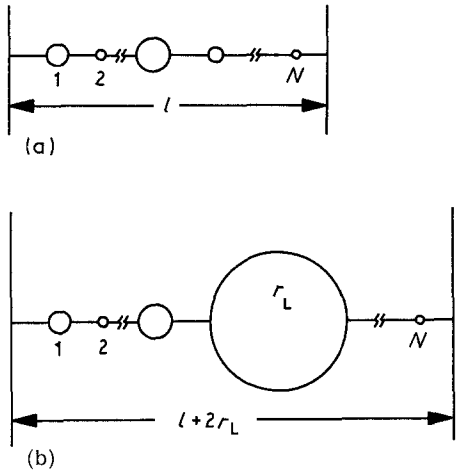

Figure 3 (a) Original pore distribution: N pores on length l. (b) Heteropore distribution: large pore with radius, r_L replaces a small pore, N pores on length $l + 2r_L$.

is ϕ_2, then Equation 1 immediately shows that

$$\phi_2 = [(l + 2r_L)/l]\phi_1 \quad (14)$$

The effect of the heteroporosity is thus mainly on the stress intensification factor.

During the densification of some heterogeneous MgO powder compacts, containing the bimodal pore distribution shown in Fig. 2a, it was observed that the constant-stress creep rate remained proportional to the densification rate while the microstructure evolved from its initial bimodal structure Fig. 2a to a more uniform one Fig. 2b: the accompanying variations in the creep rates were considerable, but paralleled the variation in the densification strain rates [24]. The results and the discussion here supports the conclusion that the anomalous change in the densification rate observed during the sintering of these MgO compacts shown in Figs 2a and 2b, should be attributed to changes in the geometrical factor ϕ, the stress intensification factor.

The stress intensification factor calculated by Beeré [14, 15] for three-dimensional powder compacts follows a relation of the form

$$\phi = \exp(aP) \quad (15)$$

where a would be a factor only dependent on the dihedral angle, and P is the fractional porosity. When the pore coordination number is high, however, as for a large pore in a fine grained matrix, then this correlation between the dihedral angle and a cannot be maintained. The two types of pores structures are shown in Figs 4a and 4b. The exponential dependence of the stress intensification factor pertains to relatively well equilibrated microstructures in which pores or pore channels are surrounded by three or four grains. With increasing pore coordination number, one could visualize that the pore geometry would correspond more and more to a random spherical one, for which $\phi \approx 1/\text{porosity}$. Then, when grain growth occurs, with a consequent transformation of the heteropore shape from a spherical one to one that is described well by the Beeré geometry, the maximum change

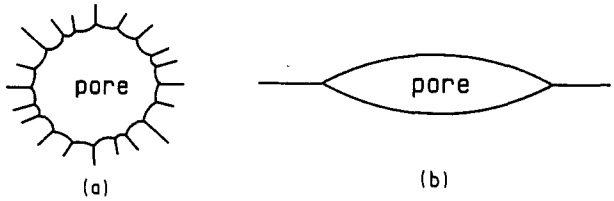

Figure 4 (a) Large spherical pore with high coordination number. (b) Lens shaped pore with low coordination number.

$\Delta\Phi_{max}$, in ϕ resulting from grain growth can be estimated to be

$$\Delta\Phi_{max} = P_L \exp(aP_L) \quad (16)$$

This factor increases with increasing heteroporosity, P_L, and decreasing dihedral angle (high value of a).

If, as in the earlier work by De Jonghe *et al* [1, 24], the large pores are initially considered to be inactive but later become active as a result of grain growth then two branches of ϕ might be observed, as sketched in Fig. 5. For the branch a, corresponding to the bimodal pore structure, one would have

$$\phi_a = \{1/(1 - P_L)\} \exp[a(P - P_L)/(1 - P_L)] \quad (17)$$

while for the later stage microstructure one has

$$\phi_b = \exp(aP) \quad (18)$$

(Equation 18 differs slightly from the one given in (1), where the correction for the porosity of the fine-pore matrix was not included.)

The data together with the corresponding microstructures reported earlier [17], generally conform to the assertion that the effects of the changes in the pore coordination number of large pores within a fine-pore matrix is chiefly on the stress intensification factor.

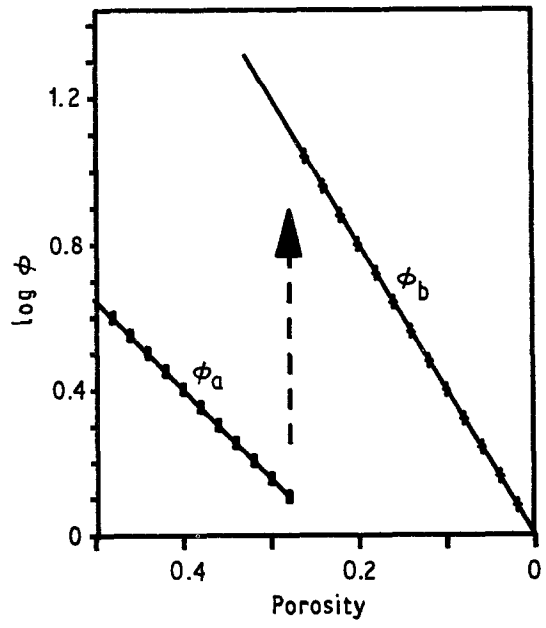

Figure 5 Two branches of ϕ corresponding to the bimodal pore structure, calculated according to Equations 17 and 18, with $a = 4$ and $P_L = 0.3$. ϕ_a corresponds to the initial value of ϕ (Equation 17) while ϕ_b corresponds to the value of ϕ after most of the heteroporosity has transformed to conform to ϕ_b (Equation 18).

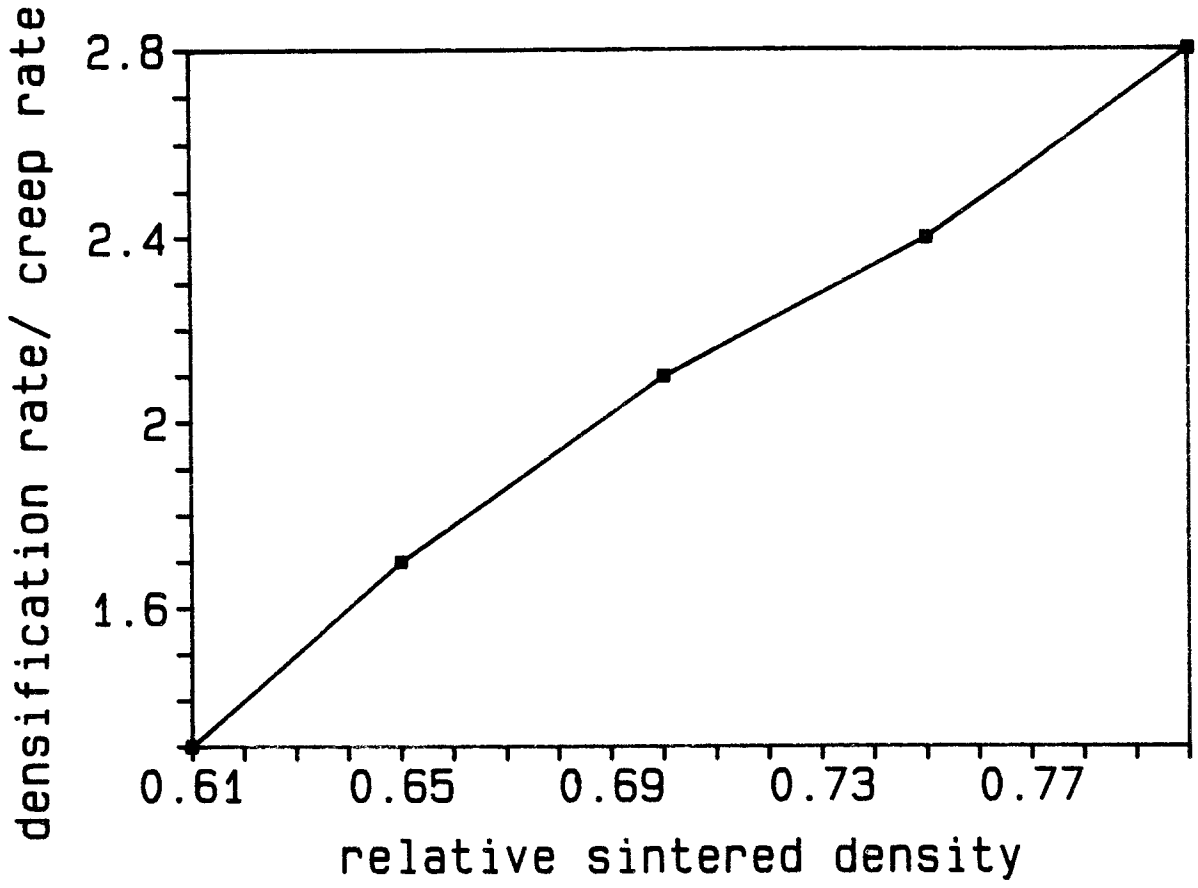

Figure 6 Densification rate over constant-stress creep rate for CdO [17], at a constant grain size of 3 μm, plotted against the sintered density.

4. Evolution of Σ/ϕ with sintered density

Numerous creep-sintering experiments [25] now are indicating that the creep strain rate over the densification rate remains relatively constant from the onset of densification to well into the final stages of sintering. The change in this ratio is usually not greater than a factor of 1.5. The relative constancy of the ratio of the densification rate to the constant-stress creep rate is a strong indication that the sintering stress, Σ/ϕ, is also relatively constant in the same sintered density range. This change is considerably less than what would be expected on the basis of the present model, as well as on the basis of other models [15] in which the sintering stress would vary significantly as densification proceeds. A near-constant sintering stress requires that the mean curvature of the pore surfaces remains constant, while the present model requires that the mean curvature increases with increasing densification. Clearly, the present model, while useful in relating the sintering stress to pore distributions and to pore coordination, does not contain those physical aspects that can predict the experimental observation of the near constancy of Σ/ϕ over a wide sintered density range.

The experimentally observed constancy of the sintering stress I/ϕ is likely to be attributable to the coarsening that occurs simultaneously with densification. Indeed, when the experimentally determined sintering stress of CdO [17] is considered grain size then, as expected from the model, a higher density compact has a higher sintering stress, as shown in Fig. 6. Near constancy of the sintering stress during densification could then prevail if the increase in the sintering stress due to densification-induced pore shrinkage and to pore coordination decrease is approximately compensated by the decrease in the sintering stress due to pore growth caused by coarsening. It would follow for systems in which coarsening is suppressed, e.g. by special choice of initial geometry or use of additives, that the sintering stress would have to increase with density. The results of Gregg and Rhines [8] on large, monosized copper spheres likely fall within this category, accounting for the difference in behaviour that the micron or submicron, non-monosized powder compacts have displayed. Further, in the conventional powder compact, a multitude of densification states are present simultaneously. The shift from open porosity to closed porosity, for example, does not take place suddenly, but develops gradually throughout the densifying compact [26]. This would also tend to average changes in the sintering stress, especially in the early sintering stages.

5. Conclusions

Examination of the densification rate of simple, stress-coupled pore assemblies indicate that the sintering stress is determined by the mean of the pore sizes weighted according to their Voronoi cell size. In correlating the sintering stress with quantitative microscopy of polished section, it is thus necessary to incorporate this additional microstructural information.

Inclusion of relatively few, large heteropores is shown to affect the effective sintering stress, Σ, very little. Instead, such pores increase the stress intensification factor.

The main effect of grain growth on the large heteropores is that they transform from a roughly spherical to a more lenticular shape, with a concommitant increase in the stress intensification factor.

The experimental constancy of the sintering stress Σ/ϕ from the onset of densification throughout a wide range of sintered densities, is argued to result mainly from a dynamic balance between pore radius decrease due to densification and pore growth due to coarsening.

Acknowledgement

This work was supported by the Division of Materials Sciences, Office of Basic Energy Sciences, U.S. Department of Energy, under Contract No. DE-AC03-76SF00098.

References

1. L. C. De JONGHE and M. N. RAHAMAN, *Acta Metall.* **36** (1988) 223.
2. F. N. RHINES and R. T. DeHOFF in "Sintering and Heterogeneous Catalysis", Materials Science Research Vol. 16, edited by G. C. Kuczynski, A. E. Miller and G. A. Sargent (Plenum Press, New York, 1984) p. 49.
3. C. H. HSUEH, A. G. EVANS, R. M. CANNON and R. J. BROOK, *Acta Metall.* **34** (1986) 927.
4. R. RAJ and R. K. BORDIA, *ibid.* **32** (1984) 1003.
5. R. T. DeHOFF, R. A. RUMMEL, H. P. LaBUFF and F. N. RHINES in "Modern Developments In Powder Metallurgy", Vol. 1 (Plenum Press, New York, 1966) p. 310.
6. G. C. KUCZYNSKI, *Met. Trans. AIME.* **185** (1949) 169.
7. P. WELLNER and EXNER, *Physics of Sintering* **5** (1973) 25.
8. R. A. GREGG and F. N. RHINES, *Metall. Trans.* **4** (1973) 1365.
9. L. C. De JONGHE and M. N. RAHAMAN, *Rev. Sci. Instrum.* **55** (1984) 2007.
10. R. L. COBLE, *J. Amer. Ceram. Soc.* **56** (1973) 461.
11. R. K. BORDIA and R. RAJ, *ibid.* **69** (1986) C-55.
12. G. W. SCHERER, *ibid.* **70** (1987) 719.
13. G. W. SCHERER, *Acta Metall.* In press.
14. W. BEERÉ, *ibid.* **23** (1975) 131.
15. *Idem., ibid.* **23** (1975) 139.
16. J. M. VIEIRA and R. J. BROOK, *J. Amer. Ceram. Soc.* **67** (1984) 245.
17. M. N. RAHAMAN, L. C. De JONGHE and R. J. BROOK, *ibid.* **69** (1986) 53.
18. W. RHODE, *ibid.* **64** (1981) 19.
19. R. L. POBER, E. A. BARRINGER, M. V. PARISH, N. LEVOY and H. K. BOWEN in "Emergent Process Methods For High-Technology Ceramics", Materials Sciences Research Vol. 17, edited by R. F. Davis, H. Palmour III and R. L. Porter (Plenum Press, New York, 1984) p. 193.
20. F. W. DYNYS and J. W. HALLORAN, *J. Amer. Ceram. Soc.* **67** (1984) 596.
21. L. C. De JONGHE, M. N. RAHAMAN and C. H. HSUEH, *Acta Metall.* **34** (1986) 1467.
22. F. F. LANGE, *J. Mater. Res.* **2** (1987) 59.
23. F. F. LANGE and B. I. DAVIS, *Adv. Ceram.* **12** (1984) 699.
24. M. LIN, M. N. RAHAMAN and L. C. De JONGHE, *J. Amer. Ceram. Soc.* **70** (1987) 360.
25. L. C. De JONGHE and V. SRIKANTH, *ibid.* **71** (1988) C-356.
26. S. C. COLEMAN and W. B. BEERÉ, *Phil. Mag.* **31** (1975) 1403.

Received 19 September 1988
and accepted 24 February 1989